This paper is a non-peer reviewed preprint submitted to EarthArXiv, which has been submitted for peer review by PNAS.

# Main Manuscript for

# Shelf invading low oxygen waters control Cenozoic organic carbon burial rates

R. E. M. Rickaby[1], T. J. Wood[1], Z. Lu[2] and C. Bjerrum[3]

[1]Department of Earth Sciences, University of Oxford, South Parks Road, Oxford OX1 3AN, UK

[2]Department of Earth and Environmental Sciences, Syracuse University, Syracuse NY 13244 USA

[3]Department of Geosciences and Natural Resource Management, University of Copenhagen, Denmark

*Rosalind E. M. Rickaby.

**Email:** rosr@earth.ox.ac.uk

**Author Contributions:** RR and ZL were involved in the conceptualization, all authors were involved in methodology, data compilation, figure composition and writing and editing of the manuscript. RR, ZL and CB were involved in funding acquisition for the work.

.

**Competing Interest Statement:** No competing interests

**Classification:** Physical Sciences; Earth, Atmospheric and Planetary Sciences

**Keywords:** Carbon cycle, sea-level, oxygen minimum zone, phosphate, ocean productivity

**This PDF file includes:**

Main Text
Figures 1 to 5

## Abstract

The thermostatic mechanisms of Earth's persistent habitability are far from resolved. High resolution C isotope records, with P accumulation and coarse fraction I/Ca over the Cenozoic, allow the recalculation and assessment of controls on the global proportional flux of organic carbon burial, a regulator of atmospheric $CO_2$ and $O_2$. Proportional $C_{org}$ burial was suppressed during the hothouse of the Eocene, coincident with an oxygenated water column and low water column phosphate. With decreased sealevel, the area for efficient organic carbon burial diminished, leading increasingly to greater water column phosphate, higher primary productivity and emergent water column de-oxygenation. The influence of sealevel on the areal extent of high sedimentation inner shelf regions acts as a control on phosphate availability for new production, respiratory demand and ocean oxygenation, as proposed by Bjerrum et al., 2006 (1). During intermediate sea-level highs of the Paleocene, and Neogene, pulses of organic carbon burial prevailed for multi-million years, in response to the redox recycling of phosphate when oxygen minimum zones with $O_2 < \sim 80$ µmol/kg were present. A self-limiting intermediate sea-level sweet spot may exist for peak $C_{org}$ burial due to redox recycling of phosphate, whereby OMZ waters with $O_2 < 80$ µmol/kg impinge on the most $C_{org}$ rich sediments of the continental shelf. This sweet spot has increasingly narrowed over Earth history due to the deepening OMZs stabilising both atmospheric $O_2$ and $CO_2$. Continental marine inundation controls on phosphate availability, and the sedimentary carbon flux, provide an inevitable positive feedback on the waxing and waning of ice sheets.

.

## Significance Statement

Unresolved mechanisms stabilise our planet's atmosphere. Combined 60 Myr reconstructions of burial rates of organic carbon and phosphorus, and water column oxygenation reveal the first order feedback between the degree of continental shelf flooding and ocean productivity. Limited P availability at high sea-level, due to efficient inner shelf burial, starved the ocean sedimentary carbon sink, oxygenated the ocean and led to $CO_2$ accumulation in the atmosphere. Lower sea-levels harboured increasing P and emergent deoxygenated waters. The extent of interaction between low oxygen zones and shelf sediments define a sea-level "sweet-spot" for rapid burial of organic carbon via redox recycling of P. The geological deepening of the OMZs led to increasing stabilisation of $CO_2$ and $O_2$ in the atmosphere of the planet.

## Introduction

### Atmospheric Composition Thermostats

Interacting redox feedbacks have rarely been considered as key drivers of atmosphere and ocean chemistry over the Cenozoic. A temperature dependent silicate weathering feedback (2) is thought to keep the sources of $CO_2$ from the outgassing of volcanoes, and from organic matter weathering, in balance with the sedimentary sinks of $CaCO_3$ and $C_{org}$. Similarly, a thermostat may regulate atmospheric $O_2$ since any increase in oxidative weathering drives an increase in the burial rate of $C_{org}$, catalysed by the redox recycling of P, which self-rectifies due to oxygenation over multimillion year timescales (3). The burial rate of organic carbon acts as a link between these two thermostats and their control on atmospheric $CO_2$ and $O_2$ by acting as a sink of carbon, and a source of oxygen to the atmosphere on long timescales (4).

On long timescales, the amount of organic carbon produced in the ocean is assumed to be limited by the availability of phosphorus, supplied by continental weathering (5). Phosphorus is an irreplaceable nutrient utilised by all organisms (6). The intimate linkage between C and P during burial, limits extended periods of $C_{org}$ burial in the past due to the efficient removal of phosphate so restricting further production of organic carbon (1). Phosphorus is buried in three main forms: Org-P, Ca-P, and Fe-P. Under anoxic bottom waters, the burial of Org-P and/or Fe-P is suppressed (7-9; reactive P pool $P_{reac}$). The ratio of carbon to phosphorus in buried organic matter ($C_{org}$/ $P_{reac}$) is ~4000 for laminated shales deposited under anoxic conditions but only ~150 for bioturbated shales deposited under oxic conditions (10). Under anoxic conditions, the reduction of iron oxy-hydroxides to ferrous iron in solution, releases phosphate (9). Consequently, phosphate recycling to the water column is greater from carbon rich sediments overlain by oxygen depleted waters (7,9,10, 11, 12).

The importance of the degree of inundation of the shelf as an amplifying feedback on climate has been considered in terms of the enhanced alkalinity of a lower sea-level ocean coined the "coral reef hypothesis" (13,14) and the impact of decreased sea level on carbon and phosphate burial during glacials (15). During low sea level more nutrients would have been transferred to the deep ocean resulting in higher phosphate concentrations and less dissolved oxygen. Bjerrum et al., 2006 (1) used hypsographic modelling to show that a sea-level decrease of order of 200 m is sufficient to change the residence time of phosphate from ~ 10 kyrs to ~50 kyrs and to more than double the average ocean P concentration due to the decreased area available for efficient C and P burial in the shallowest sediments. Such a sea-level dependence of P availability on $C_{org}$ burial is increasingly invoked to account for a significant fraction of $CO_2$ oscillation during glacial-interglacial cycles (16-18).

Here we demonstrate that the hypsographic models of ocean chemistry change due to sea-level and intimate couplings between the oxygen, phosphorus and carbon cycles are supported by data through the Cenozoic era. The sedimentary burial rate of carbon as both carbonate and organic carbon is significantly reduced during the Eocene hothouse, coincident with the period of highest atmospheric $CO_2$ and suggests that an imbalance between weathering source and sedimentary sink led to an accumulation of carbon in the atmosphere. At this time, the ocean was highly oxygenated, as evidenced from I/Ca, suggestive that an inhibited sink of carbon to the sedimentary reservoir, as a result of extended phosphate starvation, was responsible for an imbalance in the carbon cycle and the Eocene hothouse world.

## Results

### Reconstruction of Fractional Burial Rates of Organic Carbon

The size of the sedimentary organic carbon reservoir over time plays a fundamental role in the long-term oxidation of the Earth's surface environment (19). Due to the ~25 ‰ C isotopic fractionation associated with fixation of carbon via Rubisco (20,21), the carbon isotopic composition of the ocean provides a uniquely global measure of the proportional rates of $C_{org}$ burial relative to the $CaCO_3$ sink, assuming the isotopic composition of the carbon input remains constant (22). The isotopic composition of the carbon input may change due to kerogen weathering (23) or to variance in the solid earth solid earth degassing signature (24) but the near consistency of the average ocean C isotopic composition at +2‰ over geological history suggests that the input has remained largely constant even through significant perturbation in tectonism and terrestrial biota.

Mass balances of C fluxes are often calculated assuming that organic matter is buried with a $\delta^{13}C$ ~ -25 lighter than the ocean. This fractionation factor is measured in the Rubisco enzyme isolated from spinach and is not representative of algal Rubisco fractionation which may have evolved to be as small as ~ 11 ‰ (26). In order to circumvent such uncertainties in the magnitude of the fractionation associated with the diversity of affinity of Rubisco for $CO_2$ fixation, it is possible to compile a record of marine $C_{org}$ $\delta^{13}C$. A new compilation, used for the reconstruction of $pCO_2$, (27) also provides the most complete and continuous dataset of alkenone $\delta^{13}C$. Alkenone $\delta^{13}C$, has been shown to be consistently offset by 4 ‰ from the isotopic composition of the bulk cellular biomass (28) but provides an accurate measure of the $\delta^{13}C$ of marine sedimentary $C_{org}$ without contamination from terrestrial sources.

Since approximately 32 Ma, the fractionation between coccolithophore produced organic matter and oceanic DIC, has decreased from ~ 24 ‰ to ~ 16 ‰, from extrapolation of pre and post 30 Ma data to a zero intercept (Fig S1). Such a trend towards a heavier isotopic composition of marine $C_{org}$ towards the modern, is also captured at lower resolution by Hayes et al., 1999 (Fig. 1). Insight into size-dependent intracellular reservoirs of carbon (29) suggests that the alkenone producing coccolithophores have adapted on geological timescales to diminishing carbon availability by diminishing in size (30,31), with a trade off to faster division rate. This size adaptation also shrinks the internal cellular carbon pool, but keeps it full which allows a relaxation in the affinity of their Rubisco enzyme (32) with a concomitant reduction in enzymatic C isotopic fractionation (21, 33). As a result, the alkenone record, which is not species-specific, likely reflects the assemblage shift towards smaller, faster growing species with a relaxed Rubisco affinity for carbon and a diminished Rubisco fractionation factor. That the change in fractionation factor is 10 ‰ could reflect a switch in carbon substrate used from $CO_2$ to $HCO_3^-$.

The fractional flux of $C_{org}$ ($F_{Corg}$) added to marine sediments for a given interval is:

$$F_{Corg} = \left[\frac{\delta_{in} - \delta_{carb}}{\delta_{org} - \delta_{carb}}\right]$$

where $\delta_{carb}$ = $\delta^{13}C$ of carbonate deposition, $\delta_{org}$ is the $\delta^{13}C$ of $C_{org}$ deposition, and $\delta_{in}$ is the mean isotopic composition of inputs to the ocean. Although Kump and Arthur, 1997 (35) suggest the use of the shallow record of carbonate $\delta^{13}C$ for mass balance calculation, these records tend to suffer from bias and vital effects (36,37). The high resolution benthic $\delta^{13}C$ splice of Westerhold et al., 2021 (38), is used as a measure of the isotopic composition of the whole ocean.

The records of $\delta^{13}C_{org}$ and $\delta^{13}C_{carb}$ were interpolated to provide datasets at comparable resolution and age before calculation of the fractional burial of $C_{org}$. Linear regression between the fractionation and $\delta^{13}C_{carb}$ (34) suggests that $\delta_{in}$ is not well constrained by the data, hinting at a lack of steady state. $\delta_{in}$ is taken to be -4 ‰, in accord with (23) and close to the value of volcanic degassing inputs (25). For the calculation of proportional organic carbon burial rates, the input value of $\delta^{13}C_{in}$ only changes the relative burial rates and does not affect the trend. The uncertainty does not alter our results; they would be sensitive only to an undocumented time variance in this input.

The fractional burial of organic C shows a number of peaks and troughs with a multi-million year wavelength varying in amplitude, around a mean value of a fifth of the carbon sink buried as organic carbon (Fig. 2). The peaks of relative organic carbon burial are all associated with sea-level highs, but not all sea-level highs are associated with peaks of relative organic carbon burial. Most notably, although there are small steps up in the fractional organic carbon burial rate ~50 Ma, and ~ 35 Ma associated with the peaks in sealevel during this period, the amplitude of these cycles is more muted than for the sealevel highs in the early Palaeocene, and in the late Oligo-Miocene. The individual peaks in $C_{org}$ burial are supported by additional sedimentary evidence. The peak centred around 6 Myrs coincides with the “biogenic bloom” (39-41); and that around 15 Myrs with the Monterey event associated with large-scale economic reservoirs (42,43). The Paleocene-Eocene is known as a time of enhanced $C_{org}$ burial (44,45) and high inferred productivity and $C_{org}$ burial characterise the Oligo-Miocene (23 Myrs) (46). The rise in $pO_2$ associated with pulses of proportional $C_{org}$ burial, is coincident with, and could have permitted significant non-allometric shifts in brain-body size of mammals and birds in the aftermath of the K/Pg extinction during the Paleocene, and early Neogene ~ 23 Ma (47).

The Eocene suppression in proportional $C_{org}$ burial from ~ 55 Ma to 26 Ma from the average of 0.2 down to an extended period of 0.15 is also supported by the identification of "missing $C_{org}$" in Eocene marine sediments where $C_{org}$ burial was depressed by an order of magnitude compared to modern (48). Overall, our record suggests that an increase in proportional $C_{org}$ burial is generally associated with sealevel rise during the Cenozoic, except for an extended period from ~ 50 Myrs to ~ 30 Ma when the proportional burial rates are suppressed significantly. This period is characterised, in part, by some of the highest sea-levels of the last ~65 Myrs during the Eocene at over 60 m above current sea-levels.

Our reconstructed changes in $C_{org}$ burial, calculated using a methodology sensitive to global burial rates challenge earlier estimates based on sedimentary budgets (17, 49). The burial rate of $C_{org}$ is highly laterally heterogeneous and the majority of burial is constrained to narrow but areally extensive high sedimentation rate inner shelf regions. Sedimentary budgets are susceptible to regional bias and suffer from challenges in the accuracy of accumulation rates from age scales.

**Sea-level mediated phosphate and organic carbon burial**

A likely driver of the $C_{org}$ burial rate record is the sea-level dependence on the availability of phosphate (1, 50). The lowest biogenic P accumulation rates (from (51)), a measure of $P_{reac,}$ extend between 48 Ma and 30 Ma, for the same period as the lowest fractional burial rates of $C_{org}$ (Fig. 2). Increased sea-levels led to a reduced global ocean concentration of phosphate due to higher inner shelf area for efficient $C_{org}$ burial, and vice versa. A high sea-level P-limitation of global productivity therefore accounts for the first order observation of depressed $C_{org}$ burial during the highest sea-levels of the Eocene, relative to the rest of the Cenozoic, a scenario that persisted for a few millions of years.

That low biogenic P accumulation measures water column phosphate availability is well supported by an association between low biogenic P accumulation and oligotrophy. The increasing oligotrophy of the calcifying taxa through the Eocene (52) and a predominance of large heavily calcified forms (e.g. 37) characterised by low growth rates are suggestive of adaptation to low nutrient, high $CO_2$ conditions. The P accumulation rates also suggest an extended period of P limitation during the late Cretaceous. The Late Cretaceous was also dominated by phytoplankton adapted to oligotrophic conditions when sea level was thought to still be ~100 m above present (53, 54).

There is also a correlation of higher biogenic P accumulation rates (51) with periods of extended reconstructed fractional $C_{org}$ burial (Fig. 2) and higher sea-levels. The maintenance of a higher than average burial rate of $C_{org}$ for any extended multi-million year timescale is challenging due to the short residence time of dissolved inorganic phosphate in the ocean (<100 kyr but could be as short as 12-17 kyrs (11). In order to explain the apparently extended pulses of $C_{org}$ fractional burial over 3-5 Myrs accompanying sea-level highs, outside of the Eocene highstand, it is necessary to appeal to mechanisms which allow replenishment of phosphate into the water column that can then sustain prolonged multi-million year periods of $C_{org}$ burial, through effectively changing the $C_{org}$: $P_{reac}$ ratio.

The redox sensitive recycling and replenishment of phosphorus, dependent on the oxygen content of the water column (1, 7, 11, 12, 52) could maintain extended periods of $C_{org}$ deposition. The elevated $C_{org}$:$P_{reac}$ leads to more organic carbon burial per unit P delivered to the ocean. As sea-levels recede, the inner shelf area for efficient $C_{org}$ burial decreases, and oceanic P availability increases leading to a greater productivity of $C_{org}$ and a greater respiratory burden for the water column, given the lower accommodation space for burial (1). Decreased water column oxygenation therefore emerges in response to declining sea-levels and can be driven towards a threshold of oceanic oxygen concentration < ~ 80-100 μmol/kg, a key trigger for a change in phosphate behaviour. Beneath this threshold, phosphate release from sedimentary Org-P, and Fe-P is initiated. The flux of phosphate release then scales with increasingly depleted oxygen concentration such that it acts as a positive feedback, fuelling further productivity, further water column oxygen demand and even greater phosphate release. At high water column $O_2$ concentrations, phosphate is adsorbed onto iron oxyhydroxides and $C_{org}$ burial results in a low $C_{org}$/ $P_{reac}$ burial ratio with phosphate locked away in sediments.

**OMZ presence, P availability and Sea-level**

It is possible to test this mechanism of redox-sensitive recycling of P as a driver of extended $C_{org}$ burial using planktic foraminiferal I/Ca, a proxy for past water column $O_2$ concentrations (56). The principal of the proxy is that the speciation of iodine between the $I^-$ ion and the $IO_3^-$ ion is sensitive to $O_2$ availability such that the reduction of $IO_3^-$ to $I^-$ is often observed in oxygen minimum zones. It is only the $IO_3^-$ ion that substitutes for the $CO_3^{2-}$ and is incorporated into calcium carbonate fossils such as planktic foraminifera. Higher I/Ca ratios, in principle, indicate higher degrees of water column oxygenation. Existing core-top data show that planktic I/Ca decreases from >6 μmol/mol down to <3 μmol/mol in water columns containing $O_2$ beneath < 80–100 μmol/kg (57, 58); the same oxygen concentration threshold as that proposed for the anoxia-related release of reactive phosphate back to the water column. Therefore, planktic I/Ca can serve as an independent constraint on the connection between P accumulation rates and the reconstructed fractional $C_{org}$ burial (Fig. 2).

We have measured the coarse fraction (mixed species planktic foraminifera) I/Ca over the Cenozoic from Southern Atlantic Ocean (ODP Site 1262 and 1264). I/Ca is highest during the period of 30-50 Ma with values of ~ 8-10 μmol/mol and trends to lower values from 30 Ma towards the modern day with additional fluctuations above the ~ 2 μmol/mol background to values of ~ 4 μmol/mol at ~ 20, 10 and in the last 2-3 Myrs. The high iodine concentrations in the Eocene, combined with existing calibrations, suggest that the $O_2$ content of the upper water column from 30 to 48 Ma was above the 80-100 μmol/kg threshold for elevated I/Ca, qualitatively indicating that oxygen minimum zones were absent during the Eocene (Fig. 2). The decline in I/Ca beneath values of ~ 4 μmol/mol suggests that OMZs, with water column $O_2$ < 80 μmol/kg emerged and intensifed at lower sea-levels during the Paleocene, and from the Oligocene onwards.

Taking I/Ca as a measure of the oxygenation of the water column, then these records suggest an elevated water column oxygen content above the critical threshold of 80-100 μmol/kg during the Eocene. Due to the highest sea-levels from 33-48 Ma, at about 50-66 m above present day sealevel, organic carbon was most efficiently buried in the shallow high sedimentation rate waters of the inundated continental shelf, alongside the burial of reactive phosphate, leading to starvation of ocean productivity by phosphate limitation and little organic carbon for water column respiratory demand (Fig. 3) (1). Therefore the ocean harboured the lowest productivity, and the water column became highly oxygenated in accord with the N isotopic signature during Cenozoic warm periods (59).

For the rest of the Cenozoic, lower sea-levels led to a greater availability of phosphate, and so a greater proportion of increased organic carbon productivity for remineralisation and a decrease in the oxygen content of the water column. In this context, each individual period of sea-level rise on the order of 20-30m above modern, was associated with an extended multi-million year pulse of organic carbon burial, and a hint of lower I/Ca ratios (Fig. 2). This is suggestive that at these sea-levels, there was sufficient phosphate availability to drive extensive areas of the ocean close to but slightly above the threshold $O_2$ content value of ~ 80-100 μmol/kg allowing effective recycling of phosphate back into the ocean (Fig. 3). It was only over a narrow range of weathering flux of phosphate that a small increment in P input resulted in significant extended periods of $C_{org}$ burial, where the initial steady state oxygen concentration of the intermediate depth waters were close to this critical oxygen concentration (80 μmol/kg) (Fig. 4).

## Discussion

### An Organic Carbon Burial Sweet-spot

As sea-levels dropped beneath intermediate sea-levels (+20-30m compared to today) towards the modern, the ocean should become so phosphate rich that it tended towards complete anoxia with no further amplification of phosphate release (Fig. 4). The deep ocean remained largely oxic during the Cenozoic. The Cenozoic record of $C_{org}$ burial suggests that the relationship between sea-level and $C_{org}$ burial is non-linear with low $C_{org}$ burial rates at the extremes of high and low sea-level and highest burial fluxes at intermediate sea-level.

In order for phosphate to be effectively remobilised by oxygen minimum zones (OMZs) and catalyse extended periods of ocean productivity, then the OMZs must impinge on $C_{org}$ rich sediments, predominantly on the continental shelf, yielding the highest rate of redox dependent rerelease of phosphate from those organic-rich sediments (Fig. 4). With greater sea-level recession, the OMZs may drop deeper than the depths of the $C_{org}$ rich sediments of the continental shelf. This is the situation in the modern ocean, where the tops of the OMZs are largely deeper than the continental shelf (60), then P remobilisation is limited. At these lower sea-levels, with the decline in shelf area for $C_{org}$ burial, a greater proportion of carbon must be remineralised in the water column, and ultimately buried as $CaCO_3$ together with alkalinity. This results in a longer residence time of carbon (and alkalinity) in the ocean and a greater sensitivity of ocean carbon storage to physical and biological processes. In our record, the optima for OMZ coincident with $C_{org}$ rich continental shelf sediments, and propagated $C_{org}$ burial appears to be close to ~ 20-40m above sea-level (Fig. 2). At this height, the top of the OMZ is present ~100-150 m deeper than the sea-level (61), but impinges on the continental shelf (maximum depth~ -120 m) allowing a maximum of $C_{org}$ burial.

### Implications for the total sedimentary carbon sink

Given the link between P limitation of the $C_{org}$ flux to sediments, and high $CO_2$ in the atmosphere during the Eocene, it is plausible that a deceleration in the sedimentary carbon sink led to accumulation of ocean-atmosphere $CO_2$. The Eocene experienced a dearth of pelagic carbonate accumulation (62, 63; Fig S2) with an uptick in accumulation starting ~ 40 Ma, coincident with a rise in the Sr isotope curve (64) and inferred P influx (65). The pelagic carbonate vertical accumulation rate is inversely related to the $C_{org}$ burial (Fig. S2), suggestive that the pelagic flux dominates over the shelf flux at least from 40 Ma, and sea-level partitions the form of carbon buried. The deep sea carbonate accumulation rate appears responsive to P availability and excess carbon and alkalinity from shelf loss. The basin-wide pelagic flux accounting for accumulation and area above the CCD suggests a significant increase in the sedimentary carbon sink towards the modern (SI text, 63, Fig 5, Fig S3). Low resolution records suggest that the decline in tropical shelf accumulation (66) is of a similar magnitude to the increase in pelagic accumulation such that there may have been compensation between these two carbonate sinks (Fig. 5). Assuming the $CaCO_3$ sink remains constant, or is always in balance with the weathering flux, the maximum change in the proportional $C_{org}$ flux from 0.15 to 0.3 represents only ~ 20% increase in the *total* C sink, or an increase by 20% of imbalance between the sink relative to the supply. The pulsed organic carbon "burial events' persist for just 5 Myrs (Fig. 5). These short-lived increases in the C sink are beneath the threshold to drive sufficient imbalance for a runaway icehouse (67). It is likely that the P starvation of the Eocene ocean was alleviated increasingly towards the modern promoting a higher total sedimentary flux of $C_{org}$ and $CaCO_3$ and pulsed $C_{org}$ burial events. Sea-level represents a major carbon cycle feedback via its influence on the availability of P for driving the carbon sink which acts as a positive feedback both on ice sheet growth with increasing sedimentary carbon sinks, and on ice sheet retreat, with declining carbon sinks

**Negative Carbon Cycle Feedbacks**

The positive feedback between sea-level and the total carbon sink, accelerated during the periods of elevated $C_{org}$ burial rates due to the redox recycling of P at intermediate sea-levels, requires similar rate dependent negative feedbacks to rectify the system. A slow-down in weathering with cooling and and ice sheet growth, would reduce the supply of phosphate to the ocean and slow the sedimentary carbon flux. This feedback may have an upper threshold since high weathering rates at high sea-levels persistently trap phosphate in inner shelf sediments and limit the carbon sink. Increasingly high phosphate concentrations at lower sea-levels, alternatively, may inhibit both the carbonate shelf and pelagic accumulation rates. Coccolithophores grown at high phosphate decrease their calcification rate (68), because cell division becomes too fast for the diffusive carbon supply rate for calcification such that calcite/cell decreases (69,70). Since the Eocene, coccolithophores have shrunk (30), with higher growth rates (71) and lower calcification intensities (31) in concert with decreased vertical accumulation rates (Fig. S2). Pelagic carbonate accumulation rates could provide a $CO_2$ dependent feedback to the system (Figure 5, S2) with the calcification/cell paralleling the evolution of the $CO_2$:P of the ocean and slowing down the carbon sink. At very low sea-levels and in the absence of significant $C_{org}$ burial on the shelf, slow pelagic accumulation leads to a rectifying build-up of $CO_2$ in the atmosphere.

The intermediate shelf-area sweet-spot for high organic C burial rates must be inherently self-limiting due to draw-down in atmospheric $CO_2$. Cooling deepens the OMZs through the temperature dependence of remineralisation rates (72,73), or through decreased sea-level from ice sheet growth, sliding the OMZs off the continental shelf and deeper than the optimal P rerelease. Alternatively, redox P-release may be limited by a slower negative feedback due to elevated atmospheric oxygen from high organic carbon burial which reoxygenates the ocean [3, 9]; invoked to generate self-sustaining oscillations (74). This oscillation may apply to the Cenozoic cycles in proportional organic C burial, with an approximate wave length of ~5 Myrs, before and after the Eocene period of P starvation.

**Broader Implications**

The flux of carbon and phosphate to shelf sediments is an inescapable positive feedback on sea-level change, particularly during reduced continental shelf flooding and glaciation. On shorter timescales, the inundated continental shelf of the interglacial periods, yields higher $C_{org}$ burial rates, more positive $\delta^{13}C$ (74), and a natural oscillation back to a lower $CO_2$ glaciation (16, 76, 77).

The sweetspot that allows enhanced organic carbon burial for multi-millions of years through redox recycling of P requires a rather unique set of ingredients: sufficient P weathering, an $O_2$ threshold of 80-100 μmol/kg in the water column, and a depth of the $O_2$ minimum that impinges on plentiful organic rich sediments on an areally extensive (tropical) continental shelf. Significant low latitude continental land mass, tectonism (78) or life on land to accelerate P input (79) and a biological pump dominated by eukaryotes (80, 81) yielding a shallow OMZ, may be prerequisites for significant atmospheric $O_2$ build up, inevitably accompanied by significant glaciation. For any given sea-level, and phosphate supply, shallow OMZs, would have impinged at shallower depths of the continental shelf, typically containing a higher fraction of $C_{org}$ and P for redox recycling due to the high coastal sedimentation rate. Consequently, the ocean would have been more closely poised to the threshold to allow extensive $C_{org}$ burial for small changes in sea-level or perturbations to the P budget (82). With shallower OMZs, there was a much greater areal extent of the continental shelves for persistent phosphate release during sea-level retreat allowing greater redox recycling of P for longer before inhibition of the organic carbon burial cycle by build up of atmospheric oxygen. Such a mechanism speaks to the pulsed nature of $O_2$ build up and would have resulted in much higher amplitude glaciations, potentially contributing to the potential for Snowball Earth (83). Glaciations have become more muted as $O_2$ has accumulated in the atmosphere and since the deepening of the OMZs across the Mesozoic boundary (84) due to the rise of the mineralised plankton. The sweetspot for organic carbon burial has become much narrower over time, increasingly stabilising the climate and atmosphere.

## Conclusions

Records of fractional burial of $C_{org}$ are consistent with a persistent positive feedback on the size of the carbon sink as the Earth became more glaciated during the Cenozoic. The Eocene ocean was starved of P by the degree of continental shelf inundation effectively trapping the P with the highly efficient shallow $C_{org}$ burial. With declining sealevels, and reduced area of continental shelf inundation, P becomes increasingly available to the ocean, elevating the oxygen demand of the water column until the OMZs emerged in the aftermath of the Eocene/Oligocene Boundary. The presence of subsurface waters with an O2 content less than 80 µmol/kg , impinging on the $C_{org}$ rich sediments of the continental shelf may represent a rapid feedback on carbon burial. At these sea-levels, ~ 30m above modern, $C_{org}$ burial persists for timescales > 1 million years due to the redox recycling of phosphate; a scenario which is likely self-limiting. This record demonstrates that pulsed burial of organic carbon is a persistent feature of glaciated worlds. At lower sea-levels still, this rerelease of P is more limited if the OMZs are deeper than the continental shelf break; akin to the modern day. As a result, the modern ocean reflects a more anoxic water column than that experienced in the Eocene, and likely through the Mesozoic, which counterintuitively harbour the most oxygenated waters coincident with the warmest periods, and highest sea-levels. The deepening of the OMZs through time, was a key factor in stabilising the climate of the Earth system.

## Materials and Methods

### Foraminifera cleaning and I/Ca Analysis

ODP Sites are located on the Walvis Ridge with ODP Site 1262 from 27º 11.15' S 1º34.62' E, 4755 m water depth and ODP Site 1264 from 28º 31.95'S 2º 50.73' E and 2505 m water depth. 3–5 mg of coarse fraction material (>63 µm) for each sample, was weighed, crushed, and rinsed with deionized water to remove residual pore water before dissolution. A previous study (Zhou et al., 2014, Paleoceanography) showed that the coarse fraction without further cleaning by oxidative or reductive reagents was sufficient to capture the same trend in I/Ca as cleaned single genus planktic foraminiferal measurements. I/Ca was measured on a quadrupole inductively coupled plasma mass spectrometry (Bruker M90) at Syracuse University. Carbonate samples were dissolved in 3% nitric acid and diluted to form solutions with ~50 ppm Ca for analyses. Fresh calibration standards, matching the sample matrix, were prepared for every batch of samples. The precision of 127I is typically better than 1% and is not reported separately for each sample. The long-term accuracy is guaranteed by frequent repeats of the reference material JCp-1. The detection limit of I/Ca is typically below 0.1 µmol/mol. The I/Ca measurement were placed on the age model of (24).

## Acknowledgments

The project received funding from the European Research Council (ERC) under the European Union's Horizon 2020 research and innovation program (SCOOBI project, grant agreement no. 101019146; REMR) and from the Natural Environment Research Council (NERC; PUCCA project, award NE/V011049/1. Z Lu is supported by NSF EAR 2323366 and EAR 2121445. This research used samples provided by the International Ocean Discovery Program (IODP) to whom we are grateful.

**References**

1. C. J. Bjerrum, J. Bendtsen, J., J. J. F. Legarth, Modelling organic carbon burial during sea-level rises with application to the Cretaceous. *Geochem, Geophys, Geosys.* **7**, Q05008, 1-24 (2006).
2. J. C. G. Walker, P. B. Hays, J. F. Kasting, A negative feedback mechanism for the long-term stabilization of Earth's surface temperature. *J. Geophys. Res Oceans*, https://doi.org/10.1029/JC086iC10p09776 (1981).
3. P. Van Capellan, E. D. Ingall, Redox stabilization of the atmosphere and oceans by phosphorus-limited marine productivity. *Science*, **271**, 493-496 (1996).
4. Z. Lu, R. E. M Rickaby, J. L. Payne, A. N. Prow, Phanerozoic co-evolution of O2-CO2 and ocean habitability. *Nat. Sci. Rev.* **11**, nwae099 (2024).
5. R. E. Hecky, P. Kilham, Nutrient limitation of phytoplankton in freshwater environments: A review of recente evidence on the effects of enrichment. *Limnol. Oceanogr.,* **33**, 796-822 (1988).
6. C. R., Benitez-Nelson, The Biogeochemical cycling of phosphorus in marine systems. *Earth Sci. Rev.* **51**, 109-135 (2000).
7. E. Ingall, R. Jahnke, Evidence for enhanced phosphorus regeneration from marine sediments overlain by oxygen depleted waters. *Geochim. Cosmochim. Acta* **58**, 2571-2575 (1994).
8. P. Van Cappellen, E. D. Ingall, Benthic phosphorus regeneration, net primary production, and ocean anoxia: A model of the coupled marine biogeochemical cycles of carbon and phosphorus, *Paleoceanogr.* **9**, 677-692 (1996)
9. A. S., Colman, H. D. Holland, The global diagenetic flux of phosphorus from marine sediments to the oceans: Redox sensitivity and the control of atmospheric oxygen levels. in Marine Authigenesis: From Global to Microbial, edited by C. R. Glenn, L. Prévôt-Lucas, and J. Lucas, Spec. Publ. SEPM Soc. *Sediment. Geol.* **66**, 53–75 (2000).
10. E. D. Ingall, R. M. Bustin, P. Van Cappellen Influence of water column anoxia on the burial and preservation of carbon and phosphorus in marine shales. *Geochim. Cosmochim. Acta* **57**, 303-316 (1993).
11. K. C. Ruttenberg, The global phosphorus cycle, in Treatise on Geochemistry, vol. 8, edited by H. D. Holland, and K. K. Turekian, pp. 585–643, Elsevier, New York. (2003).
12. K. Wallmann, Feedbacks between oceanic redox states and marine productivity: A model perspective focused on benthic phosphorus cycling. Global Biogeochemical Cycles, 17 (3). p. 1084. DOI 10.1029/2002GB001968. (2003)
13. W. H. Berger, Increase of carbon dioxide in the atmosphere during deglaciation: The coral reef hypothesis, *Naturwissenschaften* **69**, 87–88 (1982),
14. B. N. Opdyke, J. C. G. Walker, Return of the coral reef hypothesis: Basin to shelf partitioning of $CaCO_3$ and its effect on atmospheric $CO_2$. *Geology* **20**, 733–736 (1992).
15. W. S. Broecker, Glacial to interglacial changes in ocean chemistry. *Prog. Oceanogr*. **11**, 151–197 (1982).
16. K. Wallmann, B. Schneider, M. Sarnthein, Effects of eustatic sea-level change, ocean dynamics, and nutrient utilization on atmospheric $pCO_2$ and seawater composition over the last

130 000 years: a model study. *Clim. Past* **12**, 339–375 https://doi.org/10.5194/cp-12-339-2016, (2016).
17. O. Cartapanis, D. Bianchi, S. L. Jaccard, E. D. Galbraith, Global pulses of organic carbon burial in deep-sea sediments during glacial maxima. *Nat. Commun.,* **7**, 10796, https://doi.org/10.1038/ncomms10796, (2016).
18. O. Cartapanis, E. D. Galbraith, D. Bianchi, S. L. Jaccard, Carbon burial in deep-sea sediment and implications for oceanic inventories of carbon and alkalinity over the last glacial cycle. *Clim. Past* **14**, 1819-1850 (2018)
19. J. M. Hayes, J. R. Waldbauer, The carbon cycle and associated redox processes through time. *Philos. Trans. R Soc. B Biol. Sci.* **361**, 931–950 (2006).
20. K. H. Freeman, J. M. Hayes, Fractionation of carbon isotopes by phytoplankton and estimates of ancient $CO_2$ levels. *Global Biogeochem. Cy.* **6**, 185–198, https://doi.org/10.1029/92GB00190, (1992).
21. S. Poudel, D. H. Pike, H. Raanan, J. A. Mancini, V. Nanda, R. E. M. Rickaby, P. G. Falkowski, Biophysical analysis of the evolution of substrate specificity in RuBisCO. *Proc. Nat. Acad. Sci.* **48**, 30451-30457 (2020).
22. J. M. Hayes, H. Strauss, A. J. Kaufman, The abundance of $^{13}C$ in marine organic matter and isotopic fractionation in the global biogeochemical cycle of carbon during the past 800 Ma. Chem. Geol. **161**, 103-125 (1999).
23. L. A. Derry, Closing the Geologic Carbon Cycle. *Proc. Nat. Acad. Sci.* **121**, e2409333121 (2024).
24. T. Westerhold et al., An astronomically dated record of Earth's climate and its predictability over the last 66 million years. *Science* **369**, 1383–1387 (2020). https://doi.org/10.1126/science.aba6853.
25. E. Mason, M. Edmonds, S. Turchyn, Remobilization of crustal carbon may dominate volcanic arc emissions. *Science* **357**, 290–294 (2017) https://doi.org/10.1126/science.aan5049.
26. A. J. Boller, P. J. Thomas, C. M. Cavanaugh, K. M. Scott, Low stable carbon isotope fractionation by coccolithophore RubisCO. *Geochim. Cosmochim. Acta* **75**, 7200–7207 (2011).
27. The Cenozoic $CO_2$ Proxy Integration Project (CenCO2PIP) Consortium* Toward a Cenozoic history of atmospheric $CO_2$. *Science*, **382**, eadi5177(2023) doi:10.1126/science.adi5177
28. E. B. Wilkes, R. B. Y. Lee, H. L. O. McClelland, R. E. M. Rickaby, A. Pearson, Carbon isotope ratios of coccolith–associated polysaccharides of Emiliania huxleyi as a function of growth rate and $CO_2$ concentration. Org. Geochem. **119**, 1-10 (2018).
29. N. Chauhan, R. E. M. Rickaby, Size-dependent dynamics of the internal carbon pool drive isotopic vital effects in calcifying phytoplankton. *Geochim. Cosmochim. Acta* **373**, 35-51 (2024).
30. S. Herrmann, H. R. Thierstein, Cenozoic coccolith size changes–evolutionary and/or ecological controls?, *Palaeogeogr. Palaeocl.,* **333/334**, 92–106 https://doi.org/10.1016/j.palaeo.2012.03.011, 2012.
31. B. Suchéras-Marx, J. Henderiks, Downsizing the pelagic carbonate factory: Impacts of calcareous nannoplankton evolution on carbonate burial over the past 17 million years, *Glob. Planet. Change*, **123** 97–109, https://doi.org/10.1016/j.gloplacha.2014.10.015, (2014).
32. J. N. Young, R. E. M. Rickaby, M. Kapralov, D. Filatov, Adaptive Signals in Algal Rubisco Reveal a History of Ancient Atmospheric $CO_2$. *Phil.Trans. Roy. Soc.* **367**, 483-492 (2012).
33. G. G. B. Tcherkez, G. D. Farquhar, T. J. Andrews, Despite slow catalysis and confused substrate specificity, all ribulouse bisphosphate carboxylases may be nearly perfectly optimised. *Proc. Nat. Acad. Sci.* **103**, 7246-7251 (2006).
34. D. H. Rothman, J. M. Hayes, R. E. Summons, Dynamics of the Neoproterozoic carbon cycle. *Proc. Nat. Acad. Sci.* **100**, 8124-8129 (2004).
35. L. R. Kump, M. A. Arthur, Global chemical erosion during the Cenozoic: Weatherability balances the budget in Tectonic Uplift and Climate Change, W. Ruddiman, Ed. (Plenum, New York, 1997), pp. 399–426, https://doi.org/10.1007/978-1-4615-5935-1 (1997).
36. C. Bolton, H. Stoll, Late Miocene threshold response of marine algae to carbon dioxide limitation. *Nature* **500**, 558–562 (2013). https://doi.org/10.1038/nature12448

37. L. M. Claxton, H. L. O McClelland, M. Hermoso, R. E. M. Rickaby, Eocene emergence of highly calcifying coccolithophores despite declining atmospheric $CO_2$. *Nat. Geosci.,* 1-6, (2022).
38. T. Westerhold et al., An astronomically dated record of Earth's climate and its predictability over the last 66 million years. *Science* **369**, 1383–1387 (2020).
39. L. Diester-Haass, K. Billups, & K. C. Emeis, In search of the late miocene–early pliocene "biogenic bloom" in the Atlantic Ocean (Ocean Drilling Program Sites 982, 925, and 1088). *Paleoceanography* **20**, 20. https://doi.org/10.1029/2005PA001139 (2005).
40. M. E. Gastaldello, C. Agnini, T. Westerhold, A. J. Drury, R. Sutherland, M. K. Drake, et al. The Late Miocene-Early Pliocene Biogenic Bloom: An Integrated Study in the Tasman Sea. *Paleoceanography and Paleoclimatology*, **38**, e2022PA004565. https://doi.org/10.1029/2022pa004565 (2023).
41. B.–.T. Karatsolis, B. C. Lougheed, D. De Vleeschouwer, *et al.* Abrupt conclusion of the late Miocene-early Pliocene biogenic bloom at 4.6-4.4 Ma. *Nat Commun* **13**, 353 https://doi.org/10.1038/s41467-021-27784-6 (2022).
42. E. S.C. Anttila, F. A. Macdonald, D.Szymanowski, B. Schoene, A. Kylander-Clark, C. Danhof, D. S. Jones, Timing and tempo of organic carbon burial in the Monterey Formation of the

Santa Barbara Basin and relationships with Miocene climate. *Earth and Planet Sci. Letts.* **620**, 118343 (2023). https://doi.org/10.1016/j.epsl.2023.118343.
43. L. A. Derry, C. France-Lanord, Neogene growth of the sedimentary organic carbon reservoir. *Paleoceanogr*. **11**, 267–275 (1996). https://doi.org/10.1029/95PA03839.
44. K. Kurtz, L. R. Kump, M. A. Arthur, J. C. Zachos, A. Paytan, Early Cenozoic decoupling of the global carbon and sulfur cycles. *Paleoceanogr.* 18 1-14, (2003). https://doi.org/10.1029/2003pa000908
45. N. Komar, R. E. Zeebe, G. R. Dickens, Understanding long-term carbon cycle trends: late Paleocene through the early Eocene. *Paleoceanogr. Paleoclim.,* https://doi.org/10.1002/palo.20060, (2013).
46. L. Diester-Haass, K. Billups, K. Emeis, Enhanced paleoproductivity across the Oligocene/Miocene Boundary as evidenced by benthic foraminiferal accumulation rates, *Paleogeogr., Paleoclim. Palaeoecol.* **302**, 464-473, (2011).
47. J. B. Smaers *et al.*, The evolution of mammalian brain size. *Sci. Adv.***7**, eabe2101(2021).DOI:10.1126/sciadv.abe2101
48. A. Olivarez Lyle, M. W. Lyle, Missing organic carbon in Eocene marine sediments: Is metabolism the biological feedback that maintains end-member climates, *Paleoceanogr. Paleoclim.,* https://doi.org/10.1029/2005PA001230 (2006).
49. Z. Li, Y. G. Zhang, M. Torres, B. J. W. Mills, Neogene burial of organic carbon in the global ocean. *Nature* **613**, 90–95 https://doi.org/10.1038/s41586-022-05413-6. (2023).
50. C. J. Bjerrum, J. Bendtsen, Relations between long term sea-level change, shelf-ocean exchange and shelf burial of organic material, Eos Trans. AGU, 83, Ocean Sci. Meet.Suppl., Abstract OS41G-08 (2002),
51. K. B. Follmi, The phosphorus cycle, phosphogenesis and marine phosphate-rich deposits. *Earth Sci. Rev.* **40**, 55–124 (1996).
52. J. D. Asanbe, J. Henderiks, Major shifts in Equatorial Atlantic and Pacific calcareous Nannofossil Assemblages Across the Early Eocene Climatic Optimum (EECO; 53-49 Ma). *Paleoceanogr. Paleoclim.,* https://doi.org/10.1029/2024PA005038, (2025).
53. R. M. Leckie, T. J. Bralower, R. Cashman, Oceanic Anoxic events and plankton evolution: Biotic response to tectonic forcing during the mid-Cretaceous. *Paleoceanogr. Paleoclim.*, https://doi.org/10.1029/2001PA000623 (2002).
54. S. Tozzi, O. Schofield, P. Falkowski, Historical climate change and ocean turbulence as selective agents for two key phytoplankton functional groups. *Mar. Ecol. Progr. Ser.* **274**, 123-132 (2004).
55. C. P. Slomp, J. Thompson, G. De Lange, Enhanced regeneration of phosphorus during formation of the most recent eastern Mediterranean sapropel (S1), *Geochim. Cosmochim. Acta* **66**, 1171–1184 (2002).
56. Z. Lu, H. C Jenkyns, R. E. M. Rickaby, I/Ca ratios in marine carbonate as a palaeo-redox proxy during oceanic anoxic events. *Geology* **38**, 1107-1110 (2010).
57. Z. Lu, B. A. A. Hoogakker, X. Zhou C-D Hillenbrand, E. Thomas, L. Jones; R. E. M. Rickaby, Emergence of a Southern Ocean oxygen minimum zone during glacial periods. *Nat. Commun.* **7**, doi:10.1038/ncomms11146, (2016).
58. W. Lu, A. J. Dickson, E. Thomas, R. E. M. Rickaby, P. Chapman, Z. Lu, Refining the planktic foraminiferal I/Ca proxy: Results from the Southeast Atlantic Ocean. *Geochim. Cosmochim. Acta* **287**, 318-327 (2020).
59. Auderset et al., Enhanced ocean oxygenation during Cenozoic warm periods, *Nature* **609**, 77-82 (2022).
60. J. Karstensen, L. Stramma, M. Visbeck, Oxygen mimumum zones in the eastern tropical Atlantic and Pacific oceans. *Progr. Oceanogr.* **77**, 331-350 (2008)
61. A. Paulmier, D. Ruiz-Pino, Oxygen Minimum Zones (OMZs) in the modern ocean. *Progr. Oceanogr.* **80**, 113-128, (2009).
62. G. J. A. Brummer, A. J. M. Eijden, “Blue-ocean” paleoproductivity from pelagic carbonate mass accumulation rates. *Mar. Micropal.* **19**, 99-117 (1992).

63. A. Dutkiewicz, R. D. Müller, The history of Cenozoic carbonate flux in the Atlantic Ocean constrained by multiple regional carbonate compensation depth reconstructions. Geochem. Gephys. Geosys. 23, (2002). https://doi.org/10.1029/2022GC010667

64. J. Veizer, D.Ala, K. Azmy, P. Bruckschen, D. Buhl, et al., 87Sr/86Sr, δ13C and δ18O evolution of Phanerozoic seawater. *Chem. Geol.* **161**, 59-88 (1999).

65. J. K. Caves, A. B. Jost, K. V. Lau, K. Maher, Cenozoic carbon cycle imbalances and a variable weathering feedback. *Earth Planet. Sci. Lett.* **450**, 152–163 (2016). https://doi.org/10.1016/j.epsl.2016.06.035.

66. B. N. Opdyke, B. H. Wilkinson, Surface area control of shallow cratonic to deep marine carbonate accumulation. *Paleoceanogr*. **3**, 685–703 (1988). https://doi.org/10.1029/PA003i006p00685.

67. Y. Godderis, Y. Donnadieu, B. J. W. Mills, What models tell us about the evolution of carbon sources and sinks over the Phanerozoic, *Annual Review of Earth and Planetary Sciences,* 51, https://doi.org/10.1146/annurev-earth-032320-092701 (2023).

68. Kayano K, Shiraiwa Y. Physiological regulation of coccolith polysaccharide production by phosphate availability in the coccolithophorid *Emiliania huxleyi*. *Plant Cell Physiol.* **50,** 1522-1531. doi: 10.1093/pcp/pcp097 (2009).

69. S. Gill, Q. Zhang, G. M. Henderson, R. E. M. Rickaby The physiological response of contrasting coccolithophore species to Ocean Alkalinity Enhancement. *J. Geophys. Res. Biogeosciences,* revised, 2025

70. A. Gonzalez-Lanches et al., Environmental controls on coccolithophore calcite production in the Atlantic Ocean, submitted to *Nat. Comms.* (2025).

71. K. Billups, Rickaby R. E. M., Schrag D.P., Cenozoic pelagic Sr/Ca records: Exploring a link to paleoproductivity, *Paleoceanogr*., **19**, art. no. PA3005, 2004

72. C. M. Marsay, R. J. Sanders, S. a. Henson, K. Pabortsava, E. P. Achterberg, R. S. Lampitt Attenuation of sinking particulate organic carbon flux through the mesopelagic ocean. *Proc. Natl. Acad. Sci. U.S.A.,* **112**, 1089–1094, doi:10.1073/pnas.1415311112. (2015).

73. Kwon, E. Y., F. Primeau, and J. L. Sarmiento, The impact of remineralization depth on the air-sea carbon balance. *Nat. Geosci.* **2,** 630–635, doi:10.1038/ngeo612. (2009).

74. I. C. Handoh, T. M. Lenton, Periodic mid-Cretaceous oceanic anoxic events linked by oscillations of the phosphorus and oxygen biogeochemical cycles, *Global Biogeochem. Cycles,* **17**, 1092, doi:10.1029/2003GB002039 (2003).

75. K. I. C. Oliver, B. A. A. Hoogakker, S. Crowhurst, G. M. Henderson, R. E. M. Rickaby, N. R. Edwards, H. Elderfield, A synthesis of marine sediment core □13C data over the last 150 000 years. *Clim. Past* **6**, 645-673, (2010).

76. M. Adloff, A. Jeltsch-Thommes, F. Poppelmeier, T. F. Stocker, F. Joos, Sediment fluxes dominate glacial-interglacial changes in ocean carbon inventory: results from factorial simulations over the past 780000 years. *Clim. Past,* https://doi.org/10.5194/cp-21-571-2025 (2025).

77. A. C. Fowler, R. E. M. Rickaby, E. Wolff, Exploration of a simple model for ice ages. *International Journal on Geomathematics*, DOI 10.1007/s13137-012-0040-7, (2012).

78. C. R. Walton et al. Evolution of the crustal phosphorus reservoir. *Sci. Adv.* **9**, eade6923 DOI:10.1126/sciadv.ade6923 (2023).

79. B. Peret, T. Desnos, R. Jost, S. Kanno, O. Berkowitz, L. Nussaume, Root architecture Responses: In search of Phosphate. *Plant Physiol.* **166**, 1713-1723, (2014).

80. N. J. Butterfield, Oxygen, animals and aquatic bioturbation: an updated account. https://doi.org/10.17863/CAM.21972 (2018).

81. T. M. Lenton, R. A. Boyle, S. W. Poulton, G. A Shields-Zhou, N. J. Butterfield, Co-evolution of eukaryotes and ocean oxygenation in the Neoproterozoic era, *Nat. Geosci.* **7**, 257-265 (2014).

82. A. Bachan, K. V. Lau, M. R. Saltzman, E. Thomas, L. R. Kump, J. Payne, A model for the decrease in amplitude of carbon isotope excursions across the Phanerozoic, *Am. J. Sci.,* https://doi.org/10.2475/06.2017.01 (2017).

83. P. F. Hoffman, Schrag, D. P. (2002). The Snowball Earth hypothesis: testing the limits of global change. *Terra Nova,* **14**, 129–155 (2002).

84. W. Lu, W., A. Ridgwell, E. Thomas, D.S Hardisty, G. Luo, et al., Late inception of a persistently oxygenated upper ocean, *Science*, eaar5372, DOI: 10.1126/science.aar5372 (2018).
85. Caitlyn R. Witkowski et al., Molecular fossils from phytoplankton reveal secular $P_{co2}$ trend over the Phanerozoic.Sci. Adv. **4**, eaat4556 (2018). DOI:10.1126/sciadv.aat4556
86. K. G. Miller et al. Cenozoic sea-level and cryospheric evolution from deep-sea geochemical and continental margin records. *Sci. Adv.* **6**, eaaz1346.DOI:10.1126/sciadv.aaz1346 (2020)

**Figures**

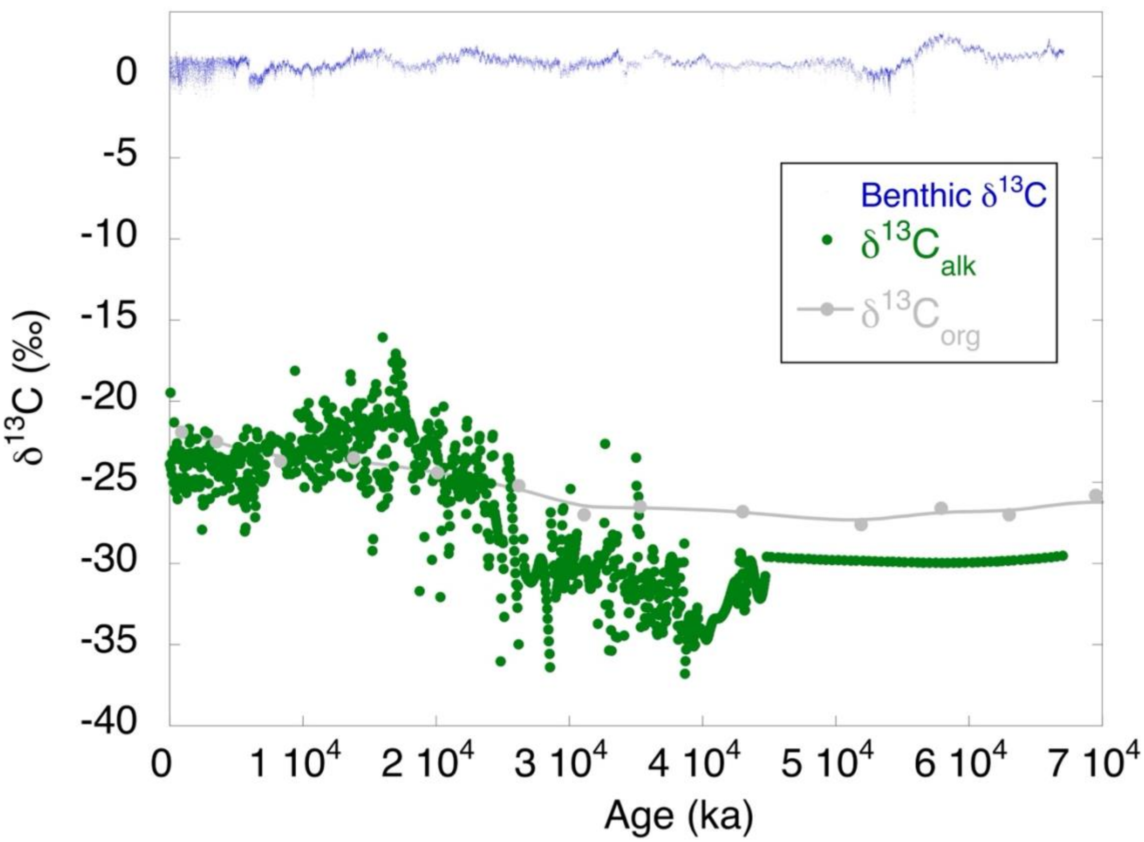


**Figure 1.** Compiled records of carbon isotopes in benthic foraminifera, blue, (24), alkenones, green, corrected for their 4.2 ‰ offset from biomass (27) including interpolated low resolution phytane (85) for the oldest parts of this record, and the longer term compilation of $\delta^{13}$C of $C_{org}$, grey, from (22) plotted as interpolated data to obtain a common timescale.

<insert page break here>

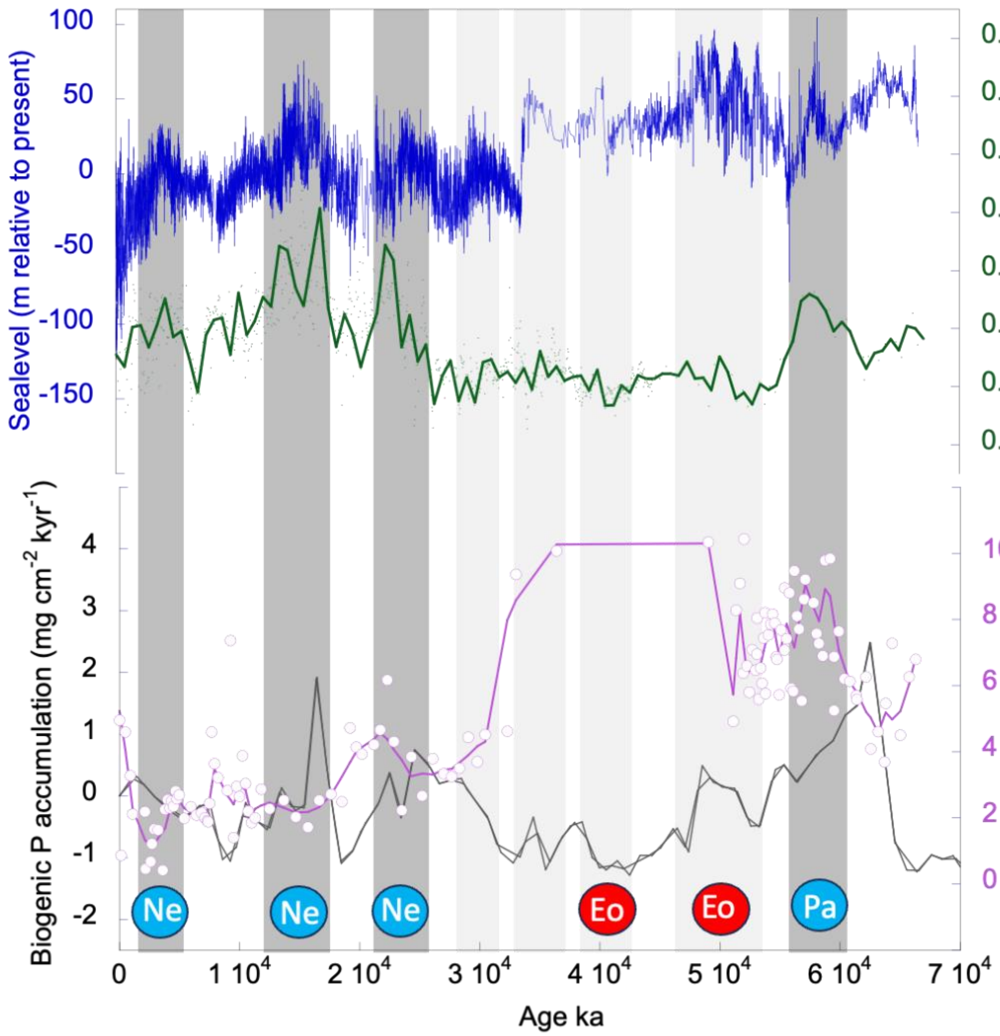


**Figure 2.** Records of sea-level (86), blue; reconstructed proportional burial flux of $C_{org}$ based on the alkenone $\delta^{13}C$ record showing small green individual datapoints and an interpolated curve; an interpolated record of I/Ca of the coarse fraction from site 1264 spliced with 1262 in the South Atlantic (open purple circles) (this study) and biogenic P accumulation in sediments with <5 wt% $Al_2O_3$, a measure of $P_{reac}$ (black, 51). The dark grey bars highlight the periods of time with higher proportional $C_{org}$ burial, higher sea-levels, higher biogenic P accumulation, and lower water column oxygen concentration. The light grey bars highlight the periods of higher sea-level fluctuations unmatched by $C_{org}$ burial. During this period, biogenic P accumulation is low and water column I/Ca is high. The red and blue circles denote the events (Paleocene Pa, Eocene Eo, and Neogene, Ne) which are then plotted on Figure 4.

<insert page break here>

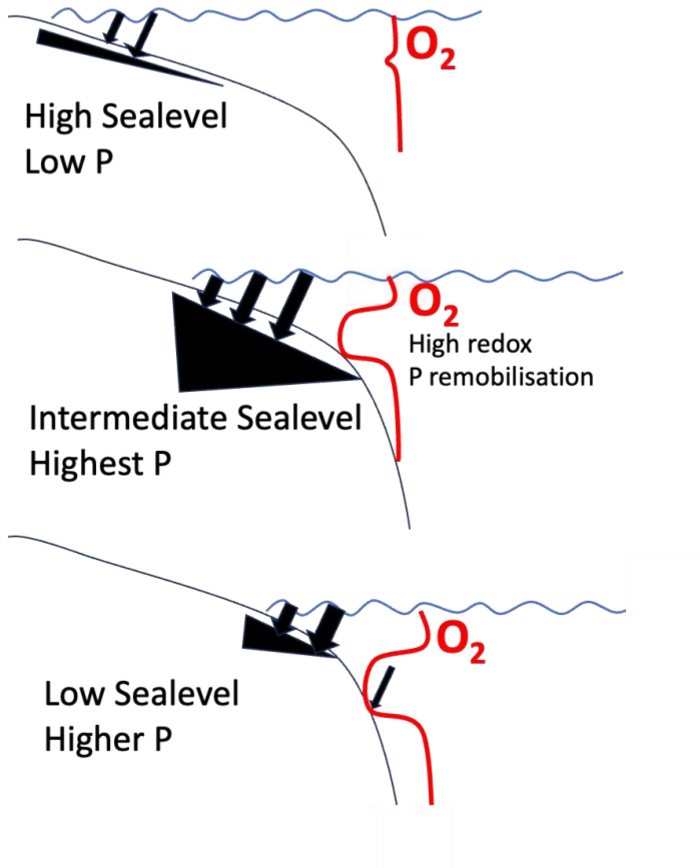


**Figure 3:** A schematic to denote the apparent sweet spot for $C_{org}$ burial. P is most efficiently buried at the highest sea-levels with the greatest area of shallow coastal sediments which restricts organic carbon production. At lower sea-levels, P is more available for the production of $C_{org}$ which increases the respiratory burden of the water column leading to the emergence of an oxygen minimum zone. At water column $O_2$ concentrations < 80 μmol/kg P rerelease is triggered which allows extensive $C_{org}$ burial. This is most effective when those minimum $O_2$ waters impinge still on the $C_{org}$ rich sediments of the continental shelf. At lower sea-levels still, the OMZs drop beneath the continental shelf, and lie in contact with much lower $C_{org}$ content sediments restricting P rerelease, as is the case in the modern ocean.

<insert page break here>

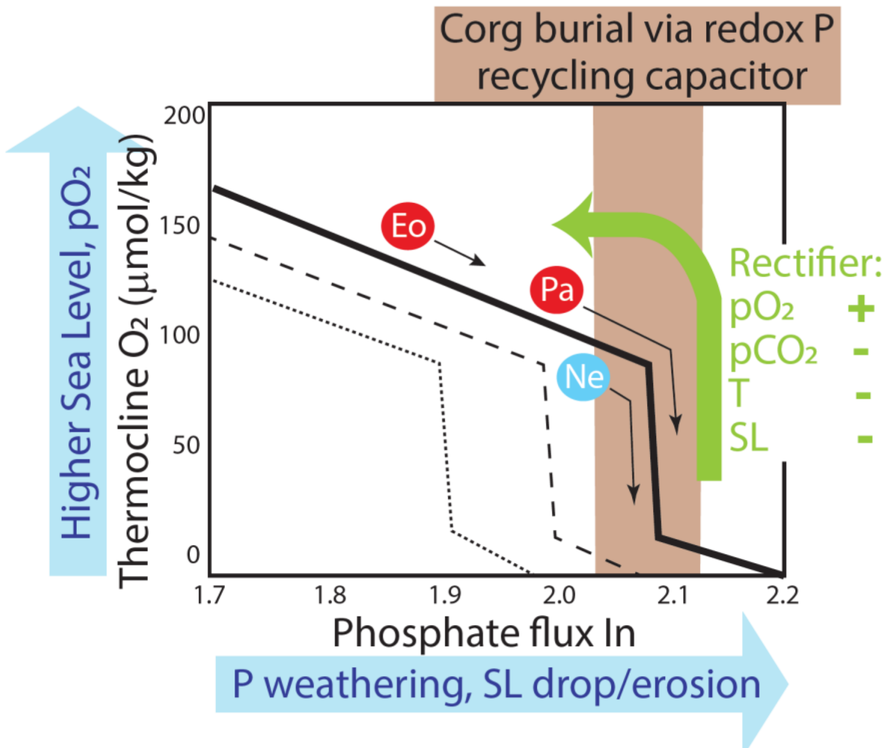


**Figure 4.** Schematic adapted from (1) to show the minimum water column oxygen concentration versus the input phosphate whereby thermocline waters close to a critical oxygen concentration (~ 80 µmol/kg), with a small additional input of P (black arrows), can lead to a threshold behaviour in $C_{org}$ burial. This critical oxygen concentration is sensitive to the weathering inputs of phosphate, which dictate the oxygen demand of organic matter produced; or to the temperature dependence of the solubility of oxygen in the water column, or to the atmospheric oxygen content. Small P increases to the ocean from erosion or residence time changes associated with sea-level rise or fall, can be amplified through the redox release of P from coastal sediments, and lead to a significant increase in organic carbon burial. Also plotted in the red and blue circles is the approximate position of the climate system before the sea-level rise events identified in Figure 2 with respect to the threshold, with arrows indicating the perturbation by a small P input. For short term perturbations, the system naturally rectifies by burying sufficient carbon to either decrease sea-level and move the OMZs off the continental shelf, or decreasing temperature which raises the $O_2$ content of the water column. On longer timescales, the build up of $O_2$ from the burial of $C_{org}$, raises the $O_2$ content of the water column and rectifies the system. Also shown, in grey, are illustrations of how the threshold may move with lower atmospheric $O_2$ contents, or much warmer water columns with lower $O_2$ concentrations due to solubility. Although this schematic suggests that the ocean tends to anoxia with even greater P input, as discussed and shown in Fig 3, it is likely that the deepening of the OMZs beyond the continental shelf represents a lower threshold to the behaviour.

<insert page break here>

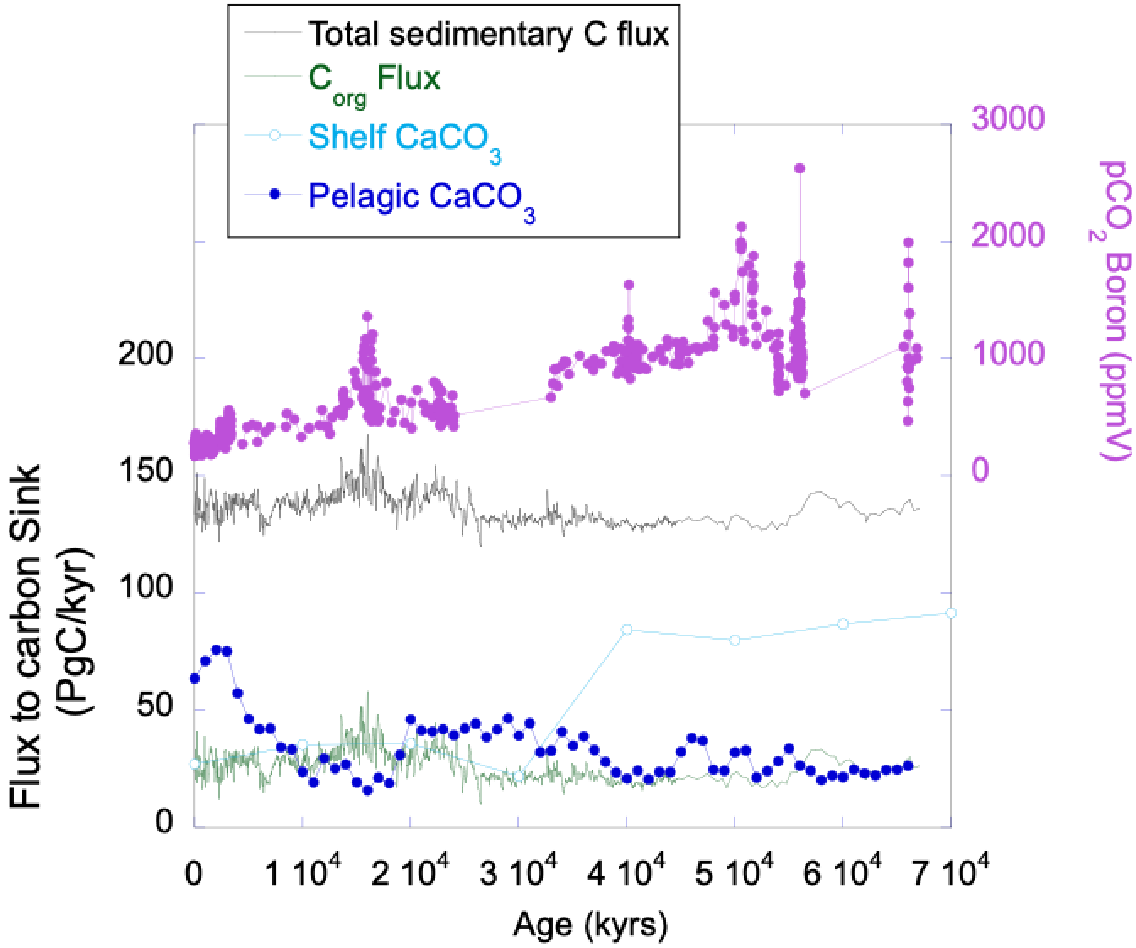


**Fig 5:** Reconstructed $pCO_2$ from B isotopes (purple dots), with calculated flux to the carbon sink in the form of shelf carbonate (light blue), Atlantic basin pelagic carbonate accounting for the area of seafloor above the CCD (dark blue, 63), and $C_{org}$ flux (dark green) from proportional burial rates and assuming that the global $CaCO_3$ flux remains constant and is compensated between the shelf and the deep ocean. The total C flux in black (SI) is a qualitative estimate since the pelagic burial rates, dominated by the Atlantic have not included the Indian and Pacific Oceans.

<insert page break here>

# Supporting Information for

# Shelf invading low oxygen waters denote sweet-spot for the organic carbon sink

R. E. M. Rickaby[1], T. Wood[1], Z. Lu[2] and C. Bjerrum[3]

*Rosalind E. M. Rickaby.

**Email:** rosr@earth.ox.ac.uk

**This PDF file includes:**

Supporting text

Figures S1 to S3

## Supporting Information Text

### Calculation of Change in Total C flux Assuming $CaCO_3$ flux remains constant

In order to translate the proportional $C_{org}$ flux into a quantitative flux, it is necessary to constrain the total flux of carbon out of the ocean. This can be done by assuming that the carbon flux out of the ocean matches that of the weathering flux into the ocean and the system is at steady state with no imbalance. This Cenozoic weathering flux has been modelled to decrease (1), increase (2) or stay approximately the same (3) over the Cenozoic and so it is hard to resolve the trend. Alternatively, it is possible to compile records of carbonate outputs from pelagic records (4) and integrate with records of shelf carbonate accumulation (5) from the degree of flooding (6) with proportion of continental shelf that is tropical and carbonate accumulating shelf, and using the long term Phanerozoic average vertical accumulation rate of ~ 25 m/Myrs (7) with 90% porosity. This calculation suggests that the total $CaCO_3$ flux, combining shelf and pelagic carbonate burial, has to a first order, remained approximately the same over the Cenozoic at ~ 110 PgC/kyrs (Fig 5) but has changed its partitioning between the shelf and the deep ocean. We note that the carbonate burial flux is likely an underestimate since it has not included a comprehensive estimate of flux and area above the CCD in the Indian and Pacific Ocean. Nonetheless the Atlantic basin accounts for the majority of carbonate burial. We have added one further figure trying to account for the Pacific fraction of $CaCO_3$ burial by scaling the burial according to the surface area of the Atlantic and Pacific Oceans (Fig. S3). There is sufficient uncertainty in these basin wide estimates, and area above the CCD at different times in Earth history that the first order assumption of total $CaCO_3$ flux staying constant or at least in balance with weathering appears most valid. The $C_{org}$ burial rate then reflects the "fast" response of the carbon cycle which can drive an imbalance between $CO_2$ source and $CO_2$ sink.

The apparent partitioning of carbon between the shelf and the deep ocean with a constant total $CaCO_3$ accumulation leads to the very simple equation that shows the implication of a change in our proportional burial for the total carbon burial sink (T):

$0.30T_1 + 0.7T_1 = T_1$
$0.15T_2 + 0.85T_2 = T_2$

If the larger proportional burial, the flux of carbonate remains constant as it is partitioned between the shelf and the deep-sea then:

$$\frac{T_1}{T_2} = \frac{0.85}{0.7} = 1.21$$

<insert page break then Fig. S1 here>

**Figures**

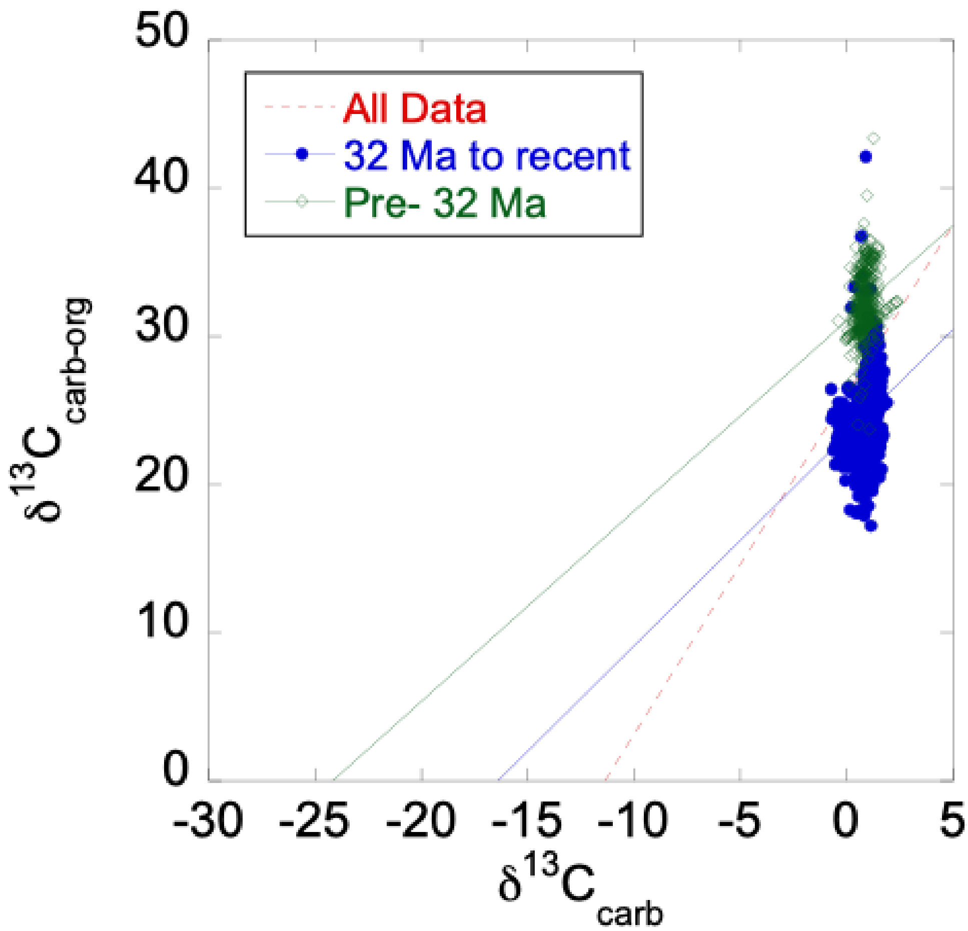


**Fig. S1.** A plot of $\delta^{13}C_{carb}$ v $\delta^{13}C_{carb-org}$ separating the data by pre (green) and post 32 Myrs (blue) compared to the whole dataset. The intercepts at $^{13}C_{carb-org}$ = 0 indicate the Rubisco fractionation factor for the different times and are suggestive that the Rubisco fractionation factor of the dominant alkenone producing phytoplankton diminished from ~ 24 ‰ to ~ 16 ‰ across the Eocene-Oligocene Boundary. That this shift is approximately ~ 10 ‰ could also imply that, coincidentally, the younger alkenone producing algae were better able to utilize the 10 ‰ heavier $HCO_3^-$ ion for photosynthesis compared to $CO_2$.

<insert page break here>

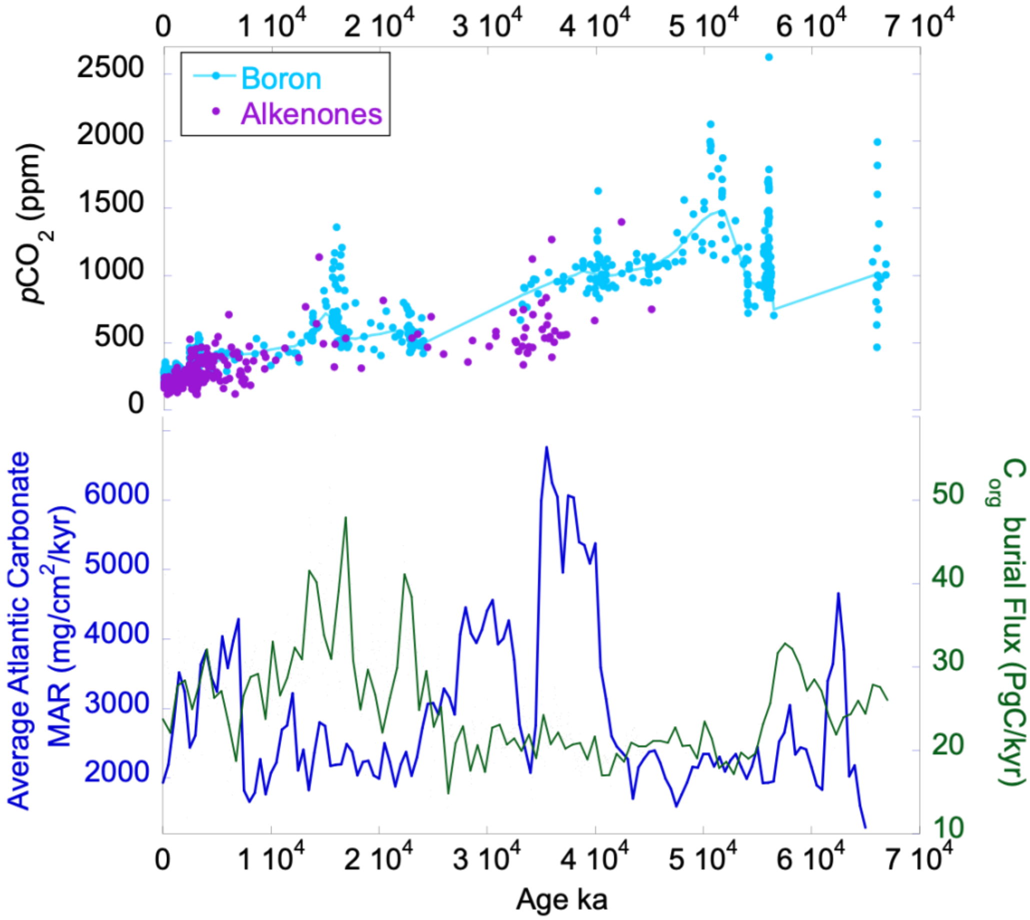


**Figure S2.** The average deep sea carbonate accumulation rate for the Atlantic compiled by (63) as a measure of carbonate productivity and vertical accumulation rate over the Cenozoic. The $CaCO_3$ mass accumulation rate (MAR) record is uncorrected for increasing area above the CCD towards the modern, plotted alongside the total Corg burial flux assuming a constant total $CaCO_3$ flux over time, and shows an inverse relationship such that the burial partitioning between different forms of carbon depends on sea-level either directly, or indirectly via the sea-level influence on P. The inverse relationship which is apparent most clearly after 40 Ma, suggests that the pelagic carbonate flux is greater than the shelf flux for that period and therefore drives the inverse relationship. Both records show low burial rates during the peak of Eocene warmth. The flux of carbonate to the sediments increases when sea-levels decrease but the magnitude of the pulse of carbonate appears to be dependent on $CO_2$ such that there are larger pulses of carbonate at times of high $CO_2$.

<insert page break here>

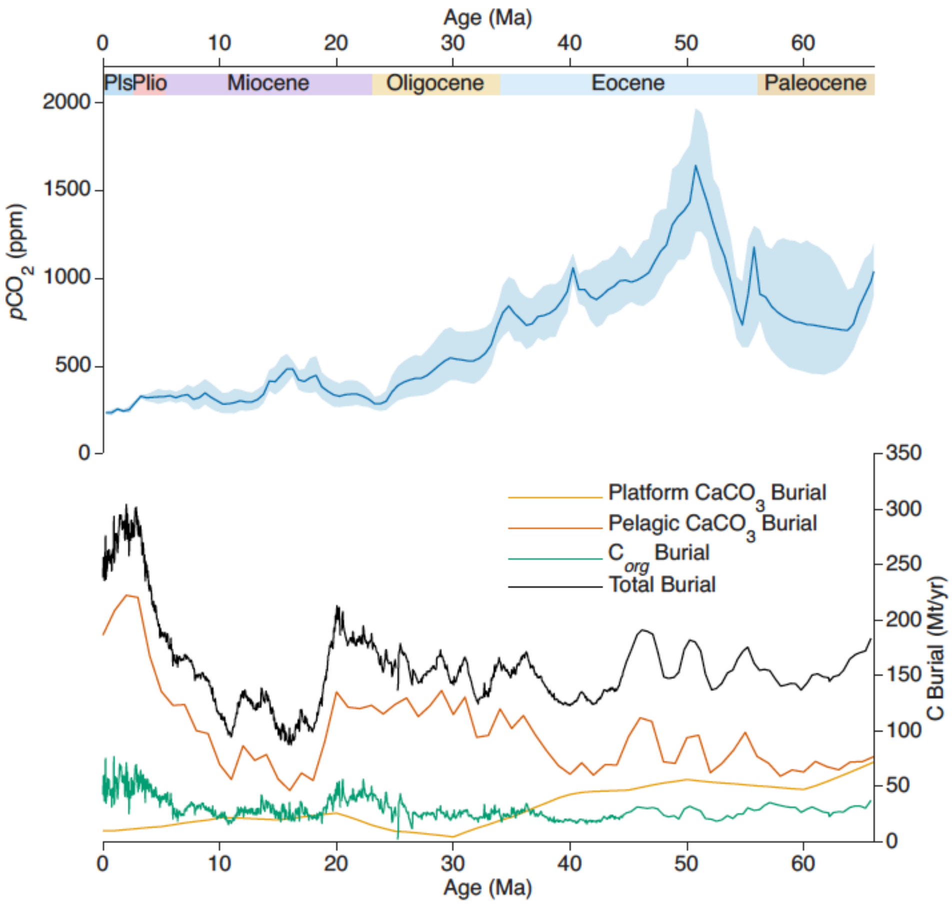


**Fig S3:** $pCO_2$ (upper panel) plotted alongside reconstructed carbon sinks, with the $C_{org}$ sink (green), the pelagic carbon burial (orange) assuming that the $CaCO_3$ flux scales with the additional surface area of the Pacific, the same assumptions as Figure 5 for the shelf burial (yellow), and calculating the total C sink (black).

<insert page break here>

**SI References**


1. A. Ridgwell, R. Zeebe, The role of the global carbonate cycle in the regulation and evolution of the Earth system, *Earth Planet. Sci. Letts* **234**,299-315 (2005).
2. G. Li and H. Elderfield, Evolution of carbon cycle over the last 100 million years. *Geochim. Cosmochim. Acta,* **103**, 11-25 (2013).
3. J. K. Caves, A. B. Jost, K. V. Lau, K. Maher, Cenozoic carbon cycle imbalances and a variable weathering feedback. *Earth Planet. Sci. Lett.* **450**, 152–163 (2016). https://doi.org/10.1016/j.epsl.2016.06.035.
4. A. Dutkiewicz, R. D. Müller, The history of Cenozoic carbonate flux in the Atlantic Ocean constrained by multiple regional carbonate compensation depth reconstructions. Geochem. Gephys. Geosys. 23, (2002). https://doi.org/10.1029/2022GC010667
5. B. N. Opdyke, B. H. Wilkinson, Surface area control of shallow cratonic to deep marine carbonate accumulation. *Paleoceanogr*. **3**, 685–703 (1988). https://doi.org/10.1029/PA003i006p00685.
6. C. M. Marcilly, Trond H., Torsvik, Clinton P. Conrad, Global Phanerozoic sea levels from paleogeographic flooding maps, Gondwana Research, Volume 110, October 2022, Pages 128-142
7. L. R. Kump, M. A. Arthur, Global chemical erosion during the Cenozoic: Weatherability balances the budget in Tectonic Uplift and Climate Change, W. Ruddiman, Ed. (Plenum, New York, 1997), pp. 399–426, https://doi.org/10.1007/978-1-4615-5935-1 (1997).